Integrated optical cross strip interferometer

M. Lohmeyer, R. Stoffer, Faculty of Mathematical Sciences, University of Twente, Enschede, The Netherlands
L. Wilkens, H. Dötsch, Department of Physics, University of Osnabrück, Osnabrück, Germany

1 Cross strip interferometer

A thick, bimodal segment of specific length and height between two single mode sections of a planar waveguide can serve as an integrated optical interferometer. It is realized by etching a wide strip from a guiding film. A — vertically guided, laterally unguided — beam of light is then made to traverse the strip perpendicularly. For a wide range of materials the structure can be dimensioned such that it shows the proper behaviour of an interferometer: Depending on the phase gain of the two modes in the thick region, the guided light interferes either almost completely destructively at the transition to the output segment, i.e. the power is radiated away into the substrate and cover regions, or constructively, i.e. most of the power passes the device. For certain applications structures of this kind can be a simple substitute for instruments like Mach-Zehnder interferometers or directional couplers. This is illustrated by two numerically simulated examples: A polarizer constructed from silicon based waveguides, which offers 34 dB polarization discrimination and 0.3 dB insertion loss with a total length of only 12 micrometers, and a proposal for an integrated magnetooptic isolator experiment, where the freedom in the lateral direction can be exploited for a proper tuning of the device.

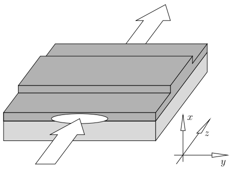

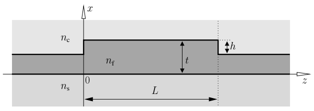

2 Overlap model

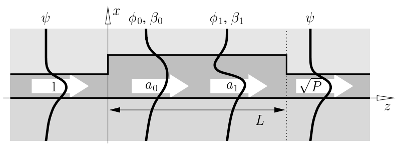

Ingredients:

ψ:	input / output mode field,
ϕ_0, ϕ_1:	fundamental and first order mode of the strip segment,
β_0, β_1:	the corresponding propagation constants,
$(\,.\,,\,.\,)$:	a suitable bilinear product.

Relative power transfer:

$$P(L) = w_0^2 + w_1^2 + 2w_0w_1\cos(\pi L/L_c)\,,$$

with $\quad a_j = (\psi, \phi_j)\,, \quad w_j = a_j^2\,, \quad L_c = \dfrac{\pi}{\beta_0 - \beta_1}\,.$

L: the length of the thick section.

Modulation range of the transmission:

$$(w_0 - w_1)^2 \le P \le (w_0 + w_1)^2\,.$$

3 Mode shapes

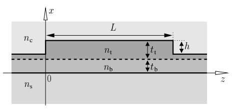

$t_b = 0.656\,\mu$m, $t_t = 0.559\,\mu$m,
$h = 0.405\,\mu$m, $\lambda = 1.3\,\mu$m,
$n_s = 1.950$, $n_b = 2.157$,
$n_t = 2.275$, $n_c = 1.0$.

TM polarization, basic magnetic field component H_y:

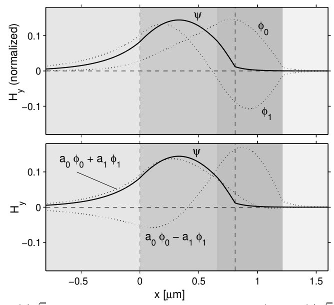

$(\phi_0 + \phi_1)/\sqrt{2} \approx \psi\,,$ $\qquad (\phi_0 - \phi_1)/\sqrt{2} \perp \psi\,.$

$a_j = 0.703, \;\; w_0 = w_1, \;\; (w_0 + w_1)^2 = 0.98$: $\qquad \min\limits_L P = 0, \quad \max\limits_L P = 0.98\,.$

4 Interferometer performance

Low losses / reflections at the input junction:

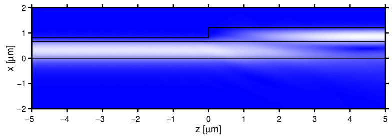

Complete constructive . . .

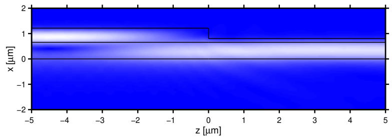

. . . or destructive interference at the output junction:

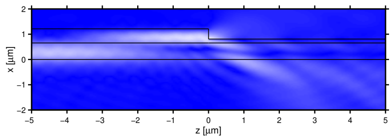

5 Transmitted and reflected power

ME: Mode expansion, 200 planar modes (guided, radiating, and evanescent) on a computational window $-15\,\mu\text{m} < x < 10\,\mu\text{m}$, hard boundary conditions.

FDTD: Finite difference time domain calculations, 400×1000 grid points, stepsizes of 10 nm, computational window $-2\,\mu\text{m} < x < 2\,\mu\text{m}$, $-5\,\mu\text{m} < z < 5\,\mu\text{m}$, absorbing boundary conditions (PML's).

Powers carried by the guided fields:

Input: ψ

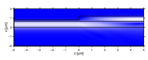

	$\psi, \rightarrow$	$\psi, \leftarrow$	$\phi_0, \rightarrow$	$\phi_0, \leftarrow$	$\phi_1, \rightarrow$	$\phi_1, \leftarrow$
ME	1	$1.1 \cdot 10^{-6}$	0.49	0	0.50	0
FDTD	1	$3.0 \cdot 10^{-5}$	0.48	0	0.51	0

Input: $(\phi_0 + \phi_1)/\sqrt{2}$

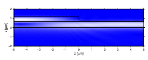

	$\phi_0, \rightarrow$	$\phi_0, \leftarrow$	$\phi_1, \rightarrow$	$\phi_1, \leftarrow$	$\psi, \rightarrow$	$\psi, \leftarrow$
ME	1/2	$2.1 \cdot 10^{-4}$	1/2	$1.1 \cdot 10^{-4}$	0.99	0
FDTD	1/2	$5.0 \cdot 10^{-4}$	1/2	$3.0 \cdot 10^{-4}$	0.99	0

Input: $(\phi_0 - \phi_1)/\sqrt{2}$

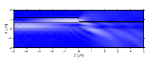

	$\phi_0, \rightarrow$	$\phi_0, \leftarrow$	$\phi_1, \rightarrow$	$\phi_1, \leftarrow$	$\psi, \rightarrow$	$\psi, \leftarrow$
ME	1/2	$2.0 \cdot 10^{-2}$	1/2	$1.3 \cdot 10^{-2}$	$6.5 \cdot 10^{-5}$	0
FDTD	1/2	$3.6 \cdot 10^{-2}$	1/2	$2.8 \cdot 10^{-2}$	$9.0 \cdot 10^{-4}$	0

6 Optimized interferometer geometries

Parameters t and h with $w_0 = w_1$ and optimum $P_{max} = (w_0 + w_1)^2$:

Cladded single layer waveguide

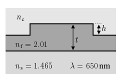

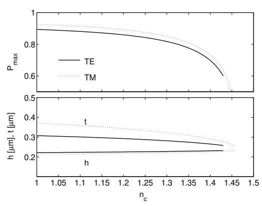

Air cladded double layer film

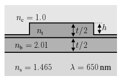

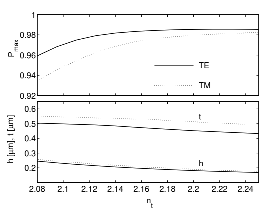

7 Polarizer

$L_c^{TE} \neq L_c^{TM}$: Adjust $L = 2m\,L_c^{TE} = (2m+1)L_c^{TM}$ with natural m.

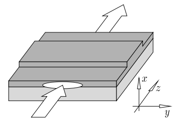

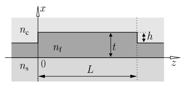

$\text{ER} = 10\log_{10} P^{TE}/P^{TM}$, $\text{LO} = -10\log_{10} P^{TE}$,
$q_0 - \Delta q \le q \le q_0 + \Delta q$: ER ≥ 20 dB, LO ≤ 1 dB.

	t	h	L	λ	n_s	n_f	n_c
q_0	$0.962\,\mu$m	$0.564\,\mu$m	$12.218\,\mu$m	$1.3\,\mu$m	1.5	2.0	1.0
Δq	9 nm	53 nm	$0.16\,\mu$m	33 nm	0.017	0.027	0.08

$P^{TE} = 93\%$, $P^{TM} = 0.035\%$, ER $= 34$ dB, LO $= 0.33$ dB,
$L_c^{TE} = 3.054\,\mu$m, $L_c^{TM} = 2.444\,\mu$m, $L = 4L_c^{TE} = 5\,L_c^{TM}$.

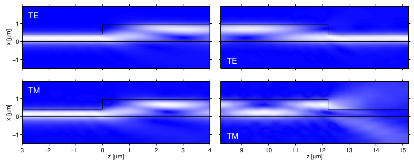

8 Isolator experiment

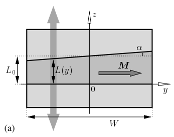

(a)

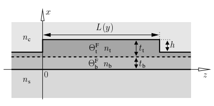

(b)

Magnetooptic interferometer; permittivity of the guiding film:

$$\hat{\epsilon} = \begin{pmatrix} n^2 & 0 & 0 \\ 0 & n^2 & 0 \\ 0 & 0 & n^2 \end{pmatrix} + \begin{pmatrix} 0 & 0 & -\mathrm{i}\xi \\ 0 & 0 & 0 \\ \mathrm{i}\xi & 0 & 0 \end{pmatrix}\,, \qquad \xi = n\lambda\Theta^F/\pi\,.$$

$W \approx 2$ cm, $\alpha \approx 0.05°$ $\qquad$ Θ^F: specific Faraday rotation.

$\boxed{\text{TM}}$ $\quad \left.\begin{matrix}\text{Forward transmission} \\ \beta_0^f, \beta_1^f, L_c^f, P^f\end{matrix}\right\} \neq \left\{\begin{matrix}\text{Backward transmission} \\ \beta_0^b, \beta_1^b, L_c^b, P^b\end{matrix}\right.$

Isolator performance for $L = 2mL_c^f = (2m+1)L_c^b$ with natural m.

	q_0	Δq
t_b	$0.656\,\mu$m	$\ge 0.2\,\mu$m
t_t	$0.559\,\mu$m	$0.16\,\mu$m
h	$0.405\,\mu$m	30 nm
L_0	5.663 mm	1.6 mm
λ	$1.3\,\mu$m	≥ 90 nm

	q_0	Δq
n_s	1.950	0.1
n_b	2.157	0.02
n_t	2.275	0.02
n_c	1.0	≥ 0.4
Θ_b^F	150°/ cm	202°/ cm
Θ_t^F	−1000°/ cm	360°/ cm

LO $= -10\log_{10} P^f$, IS $= 10\log_{10} P^f/P^b$.
$q_0 - \Delta q \le q \le q_0 + \Delta q$: Laterally shifting the beam position allows to adjust IS ≥ 20 dB, LO ≤ 1 dB ($P^f/P^b \ge 100$, $P^f \ge 0.8$).
$L_c^f = 4.5008\,\mu$m, $L_c^b = 4.4973\,\mu$m, $L_0/L_c^f \approx 1258$, $L_0/L_c^b \approx 1259$.

9 Isolator simulation

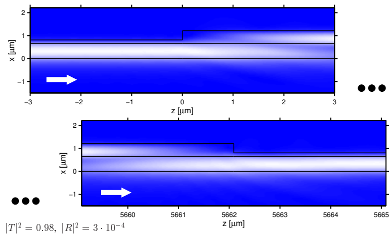

$|T|^2 = 0.98$, $|R|^2 = 3 \cdot 10^{-4}$

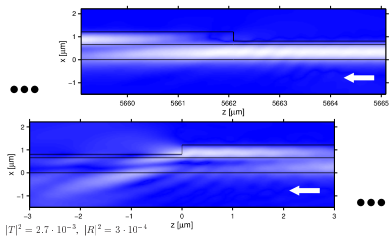

$|T|^2 = 2.7 \cdot 10^{-3}$, $|R|^2 = 3 \cdot 10^{-4}$

$P^f = 98\%$, $P^b = 0.3\%$, IS $= 26$ dB, LO $= 0.1$ dB.

Contact: Manfred Lohmeyer University of Twente, Faculty of Mathematical Sciences, Applied Analysis & Mathematical Physics Group
P.O. Box 217, 7500 AE Enschede, The Netherlands Phone: +31/53/489-3448 Fax: +31/53/489-4888 E-mail: m.lohmeyer@math.utwente.nl